Photochemical & Photobiological Sciences

Accepted Manuscript

This is an *Accepted Manuscript*, which has been through the Royal Society of Chemistry peer review process and has been accepted for publication.

Accepted Manuscripts are published online shortly after acceptance, before technical editing, formatting and proof reading. Using this free service, authors can make their results available to the community, in citable form, before we publish the edited article. We will replace this *Accepted Manuscript* with the edited and formatted *Advance Article* as soon as it is available.

You can find more information about *Accepted Manuscripts* in the Information for Authors.

Please note that technical editing may introduce minor changes to the text and/or graphics, which may alter content. The journal's standard Terms & Conditions and the Ethical guidelines still apply. In no event shall the Royal Society of Chemistry be held responsible for any errors or omissions in this *Accepted Manuscript* or any consequences arising from the use of any information it contains.

ROYAL SOCIETY OF CHEMISTRY

www.rsc.org/pps

Photochemical & Photobiological Sciences RSCPublishing

ARTICLE

Optical and electron paramagnetic resonance studies of the excited triplet states of UV-B absorbers: 2-ethylhexyl salicylate and homomenthyl salicylate

Cite this: DOI: 10.1039/x0xx00000x

Received 00th January 2012,
Accepted 00th January 2012

DOI: 10.1039/x0xx00000x

www.rsc.org/

Kazuto Sugiyama,[a] Takumi Tsuchiya,[a] Azusa Kikuchi*[a] and Mikio Yagi*[a]

The energy levels and lifetimes of the lowest excited triplet (T_1) states of UV-B absorbers, 2-ethylhexyl salicylate (EHS) and homomenthyl salicylate (HMS), and their deprotonated anions (EHS^- and HMS^-) were determined through measurements of phosphorescence and electron paramagnetic resonance (EPR) spectra in rigid solutions at 77 K. The observed T_1 energies of EHS and HMS are higher than those of butylmethoxydibenzoylmethane, the most widely used UV-A absorber, and octyl methoxycinnamate, the most widely used UV-B absorber. The T_1 states of EHS, HMS, EHS^- and HMS^- were assigned to almost pure $^3\pi\pi^*$ state from the observed T_1 lifetimes and zero-field splitting parameters. EHS and HMS with an intramolecular hydrogen bond show photoinduced phosphorescence enhancement in ethanol at 77 K. The EPR signals of the T_1 states of EHS and HMS also increase in intensity with UV-irradiation time (photoinduced EPR enhancement). The T_1 lifetimes of EHS and HMS at room temperature were determined through triplet–triplet absorption measurements in ethanol. The quantum yields of singlet oxygen production by EHS and HMS were determined by means of time-resolved near-IR phosphorescence.

Introduction

Organic UV absorbers with an intramolecular hydrogen bond have been widely used in cosmetic sunscreens. These UV absorbers enable an intramolecular excited-state proton transfer (ESPT) after photoexcitation. Intramolecular ESPT can facilitate an efficient and rapid non-radiative dissipation of the absorbed UV energy, resulting in high photostability.[1–5] This is one of the reasons why these UV absorbers are used in cosmetic sunscreens. Among these UV absorbers, 2-ethylhexyl salicylate (EHS, octyl salicylate, Neo Heliopan OS, Scheme 1) and homomenthyl salicylate (HMS, Homosalate, Scheme 1) are the first UV absorbers used in sunscreen formulations.[6,7]

The intramolecular hydrogen bonding in EHS and HMS lowers the energy of the excited state and exhibits a UV absorbance in the ideal UV-B range of 280–320 nm, while EHS and HMS have small molar absorption coefficients of <6 000 mol^{-1} dm^3 cm^{-1}.[6–8] EHS and HMS have the ability to solubilize crystalline UV absorbers such as 4-*tert*-butyl-4'-methoxydibenzoylmethane (BMDBM), the most widely used UV-A absorber in the world.[6,9] They are photostable ingredients with an excellent safety record, despite their continued use for more than 50 years.[9–11] They are approved for use in Australia, EU, Japan and USA.[12,13]

Sunscreens are photochemical systems containing more than one UV absorber to provide a perfect protection throughout the whole solar UV radiation range. There may be stabilizing or destabilizing interactions in the mixture of organic UV absorbers.[14–28] Since the lowest excited triplet (T_1) state is generally long-lived, many physical and chemical interactions are possible in the T_1 state.[29] However, to the best of our knowledge, information on the T_1 states of EHS and HMS has not yet been reported in scientific literature.

In the present study, we observed the phosphorescence and electron paramagnetic resonance (EPR) spectra of EHS and HMS and their deprotonated anions (EHS^- and HMS^-) in ethanol at 77 K. We obtained the energy levels, lifetimes and zero-field splitting (ZFS) parameters of the T_1 states. At room temperature, we observed the time-resolved triplet–triplet (T–

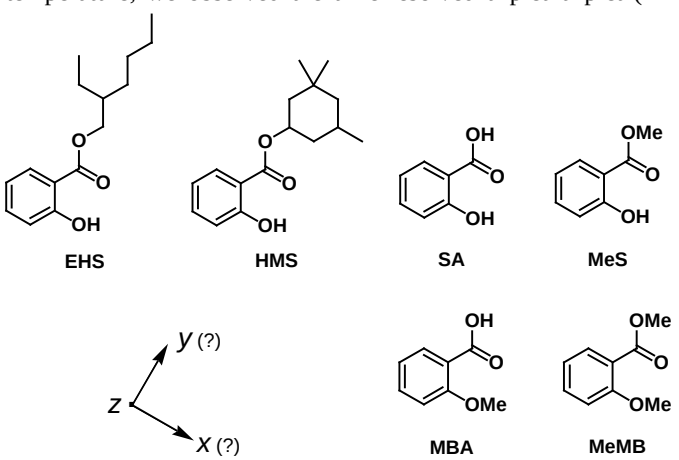

Scheme 1 Molecular structures and principal axes (x, y, z) of the ZFS tensors chosen for EHS, HMS, SA, MeS, MBA and MeMB.

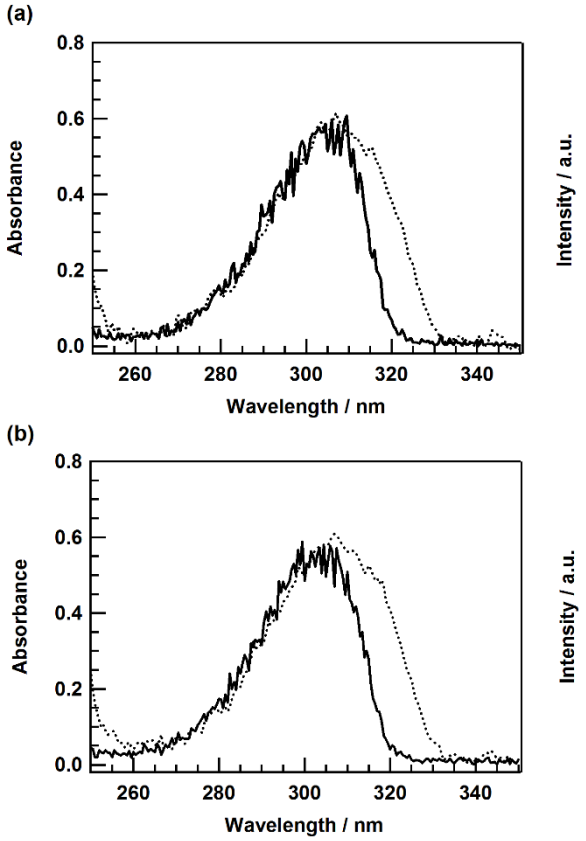

Fig. 1 UV absorption (dotted line) and phosphorescence-excitation (solid line) spectra of (a) EHS and (b) HMS in ethanol at 77 K. The sample solutions were prepared at a concentration of 1.5×10^{-2} mol dm^{-3} for the UV absorption measurements and 3.0×10^{-5} mol dm^{-3} for the phosphorescence-excitation measurements.

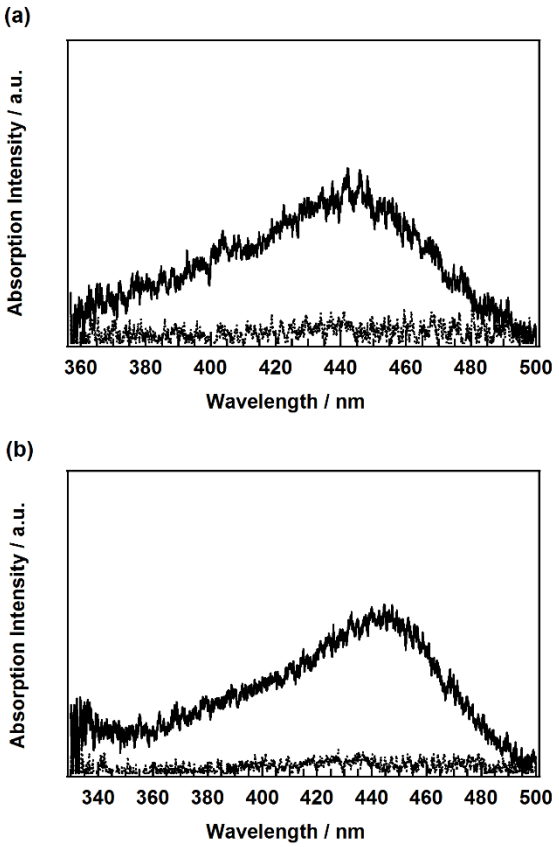

Fig. 2 Transient absorption spectra of (a) EHS and (b) HMS in Ar-saturated (solid line) and oxygen-saturated (dotted line) ethanol at 25 °C. The sampling times were set at 2–17 μs after the 266 nm YAG laser pulse. The sample solutions were prepared at a concentration of 3.8×10^{-3} mol dm^{-3} (absorbance at 266 nm was 1.0).

T) absorption spectra of EHS and HMS and the time-resolved near-IR emission spectra of singlet oxygen generated by photosensitization with EHS and HMS. In the course of the study, photoinduced phosphorescence enhancement was observed for EHS and HMS in rigid solutions at 77 K. The nature of the T_1 states of EHS and HMS is discussed. The T_1 states of salicylic acid (SA), methyl salicylate (MeS), 2-methoxybenzoic acid (MBA) and methyl 2-methoxybenzoate (MeMB) have been studied for comparison.

Experimental

Chemicals

EHS (>98%), HMS (>98%), MeS (>99%), MBA (>98%) and MeMB (>99%) were purchased from TCI and used without further purification. SA (Wako, >99.5%), ethanol (Wako, Super Special Grade) and 2,2,2-trifluoroethanol (Wako, >98.5%) were used without further purification. The concentrations shown in this study were determined at room temperature. The concentrations should be corrected for shrinkage of the solution upon freezing at 77 K.

Optical and EPR measurements

The UV absorption, total emission, phosphorescence and phosphorescence-excitation spectra at 77 K were measured by the same method as described previously.[30,31] The experimental setup for the time-resolved T–T absorption experiments is the same as that previously reported.[32] The sample solution was flowed in a Tosoh T-57-UV-10 cuvette (10 mm optical path length) for the T–T absorption spectrum measurements. For the T–T absorption decay measurements, sample solutions were deaerated by freeze–pump–thaw cycles.

The time-resolved near-IR emission measurements were carried out in ethanol. Samples were excited with a Continuum Surelite Nd:YAG laser (266 nm, repetition rate 10 Hz). The experimental setup for the time-resolved near-IR emission experiments is the same as that reported previously.[32]

The EPR spectra were measured in ethanol at 77K by a JEOL-JES-FE1XG X-band spectrometer (ν = 9210 MHz). The static magnetic field was calibrated with an Echo Electronics EFM-2000 proton NMR gauss meter. Samples were excited with a Canrad-Hanovia Xe-Hg lamp(1 kW run at 500 W) equipped with an Asahi Technoglass UV-D33S glass filter (transmits the wavelength 250–400 nm) and an Asahi Spectra REX-250 Hg lamp (250 W) equipped with an interference filter (313 nm).

Results and discussion

UV absorption spectra

The UV absorption spectra of EHS and HMS were measured in ethanol at 25 °C and 77 K. The spectra show blurred vibrational

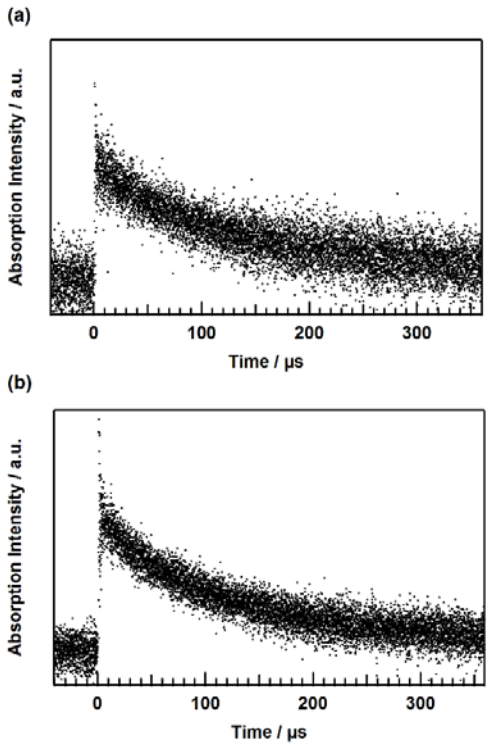

Fig. 3 Time profiles of the transient absorption of (a) EHS and (b) HMS in deaerated ethanol at 25 °C. Transient absorption was monitored at 430 nm. The sample solutions were prepared at a concentration of 3.8×10^{-3} mol dm^{-3}.

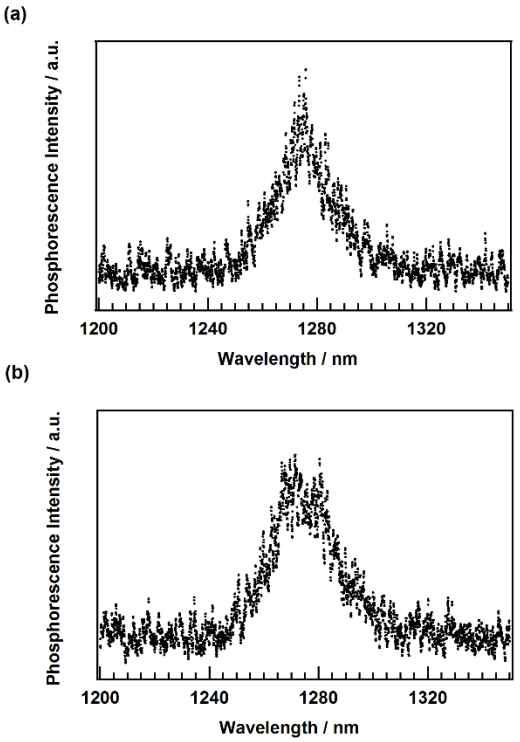

Fig. 4 Time-resolved near-IR phosphorescence spectra of singlet oxygen, $^1O_2(^1\Delta_g)$, generated by excitation of (a) EHS and (b) HMS in oxygen-saturated ethanol with 266 nm YAG laser pulses at 25 °C. The sampling times were set at 10–25 μs after the laser pulse. Inset: the phosphorescence intensity was monitored at 1274 nm. The sample solutions were prepared at a concentration of 3.8×10^{-3} mol dm^{-3}.

structure and only one peak in the UV-B range even at 77 K, as shown in Fig. 1. The molar absorption coefficients of EHS and HMS in ethanol at 25 °C were obtained to be 4 650 mol^{-1} dm^3 cm^{-1} at 306 nm and 4 580 mol^{-1} dm^3 cm^{-1} at 306 nm, respectively.

Transient absorption spectra

To obtain the information of the triplet states at room temperature, the transient absorption spectra of EHS and HMS were measured by utilizing laser flash photolysis in ethanol at 25 °C. Fig. 2 shows the transient absorption spectra of EHS and HMS in Ar-saturated ethanol obtained 3–8 μs after the 266 nm laser pulse. Fig. 3 shows the time profiles of the transient absorption signals of EHT and DBT. The decay of transient absorbance was drastically accelerated by addition of ground-state oxygen, $^3O_2$. The observed transient spectra can be reasonably assigned to T–T absorption spectra since $^3O_2$ is a well-known triplet quencher.[29] The T–T absorption decays were exponential, and the lifetimes of the T_1 states of EHS and HMS were estimated to be 140 μs and 120 μs in deaerated ethanol at 25 °C, respectively. It should be mentioned that the lowest excited singlet (S_1) states of EHS and HMS undergo intersystem crossing to the T_1 states in some degree, even though intramolecular ESPT facilitates the internal conversion of the S_1 states into the ground states.

Time-resolved near-IR phosphorescence spectra of singlet oxygen

Interaction of an excited triplet state of an organic molecule with $^3O_2$ generally leads to the sensitized formation of singlet oxygen, $^1O_2(^1\Delta_g)$.[29] The near-IR phosphorescence spectra of $^1O_2(^1\Delta_g)$ generated by photosensitization with EHS and HMS were measured in oxygen-saturated ethanol at 25 °C, as shown in Fig. 4. The phosphorescence peak was observed at 1274 nm. The lifetimes of $^1O_2(^1\Delta_g)$ generated by excitation of EHS and HMS were determined to be 15.0 μs and 14.7 μs, respectively. The observed wavelength of the phosphorescence peak is very close to that observed in ethanol by Schmidt (1273 nm).[33] The observed lifetimes are close to those observed in ethanol by Shimizu *et al.* (14.5 μs) and Kikuchi *et al.* (16 μs).[34,35]

The quantum yields of $^1O_2(^1\Delta_g)$ generation, Φ_Δ, were determined relative to phenalenone in oxygen-saturated ethanol. Φ_Δ values generated by phenalenone were reported to be almost unity in many solvents including methanol.[36,37] The Φ_Δ values of both EHS and HMS were determined to be 0.019.

Photoinduced phosphorescence enhancement

The phosphorescence spectra of EHS and HMS were measured in ethanol at 77 K, as shown in Fig. 5 and 6. The energy levels of the T_1 states of both EHS and HMS were estimated to be 27 000 cm^{-1} from the shorter wavelength edge of the phosphorescence. The phosphorescence lifetimes of EHS and HMS were observed in ethanol at 77 K. The results are given in Table 1. The energy levels of EHS and HMS are higher than those of BMDBM (E_{T_1} = 20 400 cm^{-1}) and the most widely used UV-B absorber, octyl methoxycinnamate (OMC, E_{T_1} = 19 500 cm^{-1}).[30,38] EHS and HMS may act as an triplet energy donor for BMDBM and OMC in the mixtures of UV absorbers.

In the course of the emission studies, a marked increase in the phosphorescence intensity during the photoexcitation was

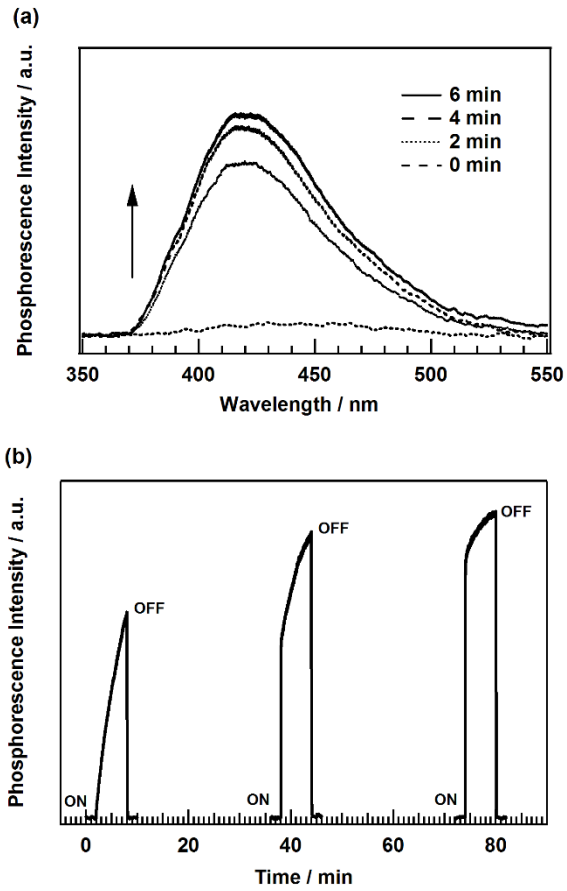

Fig. 5 (a) Phosphorescence spectra of EHS at irradiation times of 0 min, 2 min, 4 min and 6 min in ethanol at 77 K (λ_{exc} = 313 nm). (b) Irradiation time dependence of phosphorescence intensity of EHS and relaxation in the dark period of 30 min in ethanol at 77 K. Phosphorescence was monitored at 420 nm. The sample solutions were prepared at a concentration of 1.5×10^{-2} mol dm^{-3}.

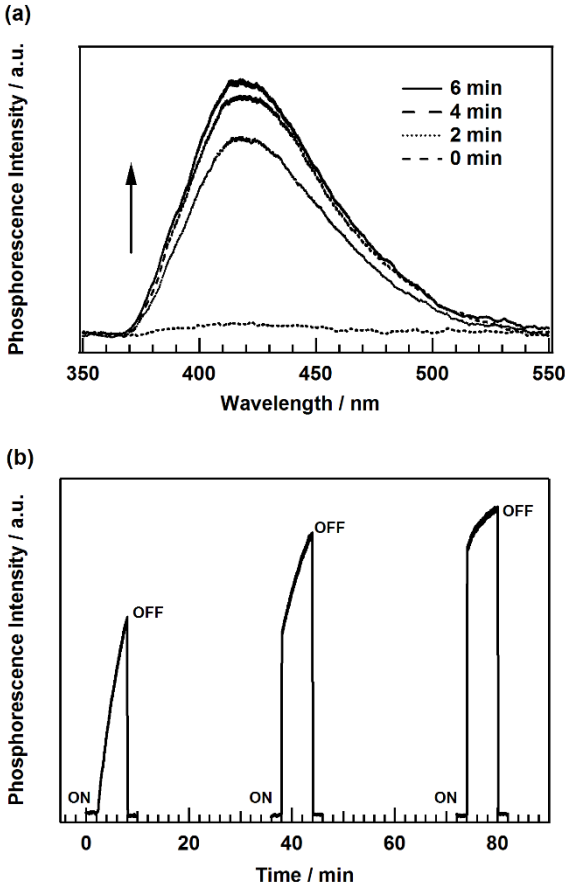

Fig. 6 (a) Phosphorescence spectra of HMS at irradiation times of 0 min, 2 min, 4 min and 6 min in ethanol at 77 K (λ_{exc} = 313 nm). (b) Irradiation time dependence of phosphorescence intensity of HMS and relaxation in the dark period of 30 min in ethanol at 77 K. Phosphorescence was monitored at 420 nm. The sample solutions were prepared at a concentration of 1.5×10^{-2} mol dm^{-3}.

observed for EHS and HMS. Fig. 5a shows the irradiation time dependence of phosphorescence intensity of EHS in ethanol at 77 K. The phosphorescence intensity rose and approached an equilibrium value (*photoinduced phosphorescence enhancement*). After a dark period of 30 min the phosphorescence intensity decreased with respect to the value from the end of the preceding irradiation period (*relaxation*). Fig. 5b shows this behavior. The phosphorescence spectrum did not change during the irradiation, as shown in Fig. 5a. The photoinduced phosphorescence enhancement and relaxation were also observed for HMS, as shown in Fig. 6.

The phosphorescence-excitation spectra of EHS and HMS are blue-shifted with regard to the UV absorption spectra, as shown in Fig. 1. The phosphorescence and phosphorescence-excitation spectra of SA, MeS, MBA and MeMB were observed in ethanol at 77 K for comparison. The results are shown in Fig. S1–S5. The observed phosphorescence spectra of MeS and MeMB are similar to those reported by Aleksiejew and Heldt.[39] The observed phosphorescence-excitation spectrum of MBA is similar to the UV absorption spectrum of MBA, although the phosphorescence-excitation spectrum is somewhat red-shifted with regard to the UV absorption spectrum, as shown in Fig. S5. The phosphorescence intensity of MBA did not increase during the excitation in ethanol at 77 K. This phosphorescence behavior was also observed for MeMB in ethanol at 77 K. The methoxy derivatives of SA where the hydroxyl groups are replaced by methoxy groups showed constant intense phosphorescence during the excitation. On the other hand, the observed phosphorescence-excitation spectra of SA and MeS are blue-shifted compared to the UV absorption spectra and the photoinduced phosphorescence enhancement was observed.

The photoinduced phosphorescence enhancement observed for EHS, HMS, SA and MeS are similar to that observed for benzophenone derivatives used as UV absorbers, 2-(2-hydroxy-4-methoxyphenyl)-4,6-diphenyl-1,3,5-triazine (HMPDT) and 2-hydroxypropiophenone at 77 K.[31,40–42] The photoinduced phosphorescence enhancement was explained by considering the intramolecular and intermolecular hydrogen bonds.[31,40–42]

One possible explanation for the observed phosphorescence enhancement is that the photoinduced intermolecular hydrogen-bond formation between EHS and ethanol leads to the enhancement of the $S_1 \rightarrow T_1$ intersystem crossing. Before excitation EHS is the closed form with a chelate-type intramolecular hydrogen bridge in ethanol. For the closed form of EHS an intramolecular ESPT takes place after excitation. This is followed by rapid internal conversion and no phosphorescence is observed at the very beginning of the first irradiation. In ethanol the fraction of the intermolecular hydrogen-bridged species to the solvent (open form) increases

Table 1 T_1 energies (E_{T_1}), phosphorescence quantum yields (Φ_P), zero-field splitting parameters (D^*) and T_1 lifetimes (τ) observed in rigid solutions at 77 K

Molecule	Host	E_{T_1} (cm^{-1})	Φ_P	D^* (cm^{-1})	τ_P (s) [a]	τ_{EPR} (s) [b]
EHS	EtOH	26 700	0.054	0.1340	1.02	1.07
EHS^-	EtOH–KOH	23 900	0.17	0.0819	0.57	0.59
HMS	EtOH	26 700	0.049	0.1350	1.01	1.01
HMS^-	EtOH–KOH	23 900	0.16	0.0834	0.58	0.59
SA	EtOH	27 000	– [c]	0.1339	0.95	0.91
SA^-	EtOH–KOH	23 700	– [c]	0.0819	0.71	– [d]
MeS	EtOH	26 700	0.048	0.1350	1.07	1.02
MeS^-	EtOH–KOH	23 900	0.27	0.0833	0.61	0.57
MBA	EtOH	26 900	0.37	0.1360	1.02	0.99
MBA^-	EtOH–KOH	26 800	0.36	0.1380	0.40	0.41
MeMB	EtOH	26 700	0.36	0.1350	1.12	1.10

[a] Obtained from the decay of phosphorescence. [b] Obtained from the decay of the EPR B_{min} signal. [c] Not available due to weak phosphorescence. [d] Not available due to weak EPR B_{min} signal.

during irradiation and the S_1 state of the open-form EHS undergoes intersystem crossing to the T_1 state. The open-form EHS in the ground state undergoes relaxation to the closed form during the dark period.

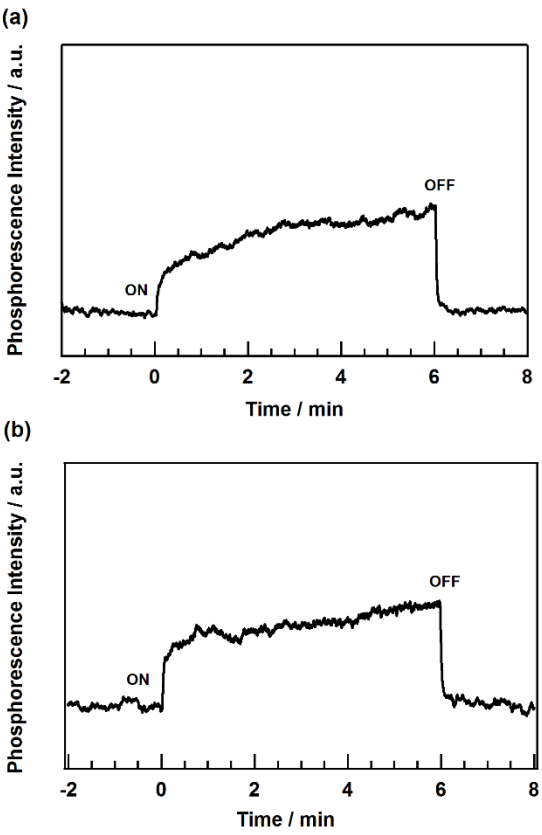

Fig. 7 (a) Irradiation time dependence of phosphorescence intensity of (a) EHS and (b) HMS in trifluoroethanol at 77 K (λ_{exc} = 313 nm). Phosphorescence was monitored at 420 nm. The sample solutions were prepared at a concentration of 1.5×10^{-2} mol dm^{-3}.

To confirm the mechanism of the observed phosphorescence enhancement the irradiation time dependence of phosphorescence intensity was observed for EHS in 2,2,2-trifluoroethanol at 77 K. As shown in Fig. 7a, phosphorescence was observable at the very beginning of the first irradiation and the phosphorescence intensity increased with the irradiation time. Before irradiation EHS is the mixture of the closed form and open form since trifluoroethanol has a stronger tendency to form hydrogen bridging than ethanol. This irradiation time dependence of phosphorescence intensity was also observed for HMS, as shown in Fig. 7b.

The phosphorescence measurements were carried out for the deprotonated anions of EHS and HMS (EHS^- and HMS^-) in ethanol–KOH at 77 K. The results are listed in Table 1. As is clearly seen in Fig. 8, the phosphorescence spectra of EHS^- and HMS^- are red-shifted with regard to those of their neutral forms. The phosphorescence intensity of EHS^- and HMS^- did not increase during the excitation. These experimental results also support the above-mentioned mechanism of the observed phosphorescence enhancement for EHS and HMS. The phosphorescence lifetimes of the compounds studied were determined in ethanol at 77 K and are listed in Table 1. The observed phosphorescence lifetime of MBA is close to that observed in EPA (ether–isopentane–alcohol, 5:5:2 by volume) at 77 K (0.96 s).[43]

The quantum yields of phosphorescence, Φ_P, of EHS and HMS were determined relative to the quantum yields of fluorescence, Φ_F, of 9,10-diphenylanthracene in ethanol at 77 K, Φ_F = 1.0.[44,45] In the same manner as reported previously,[46,47] the values of Φ_P were determined to be 0.054 and 0.049 for EHS and HMS, respectively, after the phosphorescence intensity reached equilibrium value. The Φ_P values of the compounds studied are listed in Table 1. MBA and MeMB without intramolecular ESPT are strongly phosphorescent as expected.

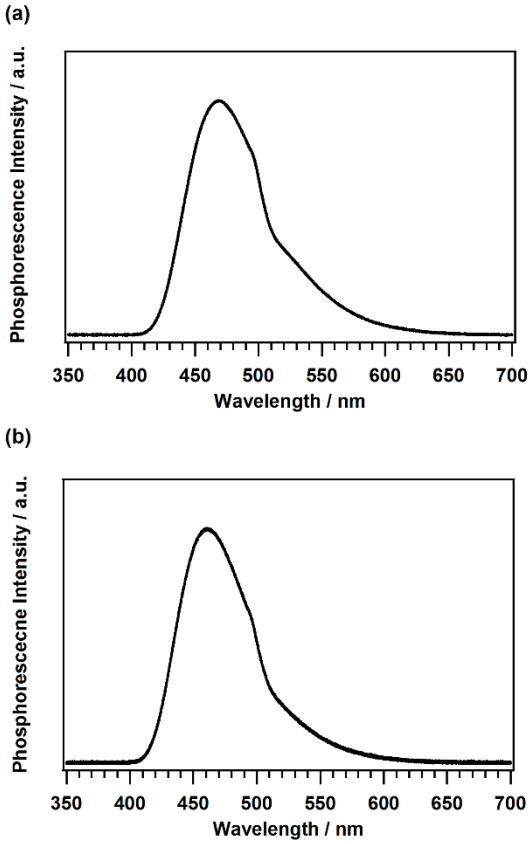

Fig. 8 Phosphorescence spectra of (a) EHS^- and (b) HMS^- in ethanol–KOH at 77 K (λ_{exc} = 334 nm). The sample solutions were prepared at a concentration of 1.5×10^{-4} mol dm^{-3}.

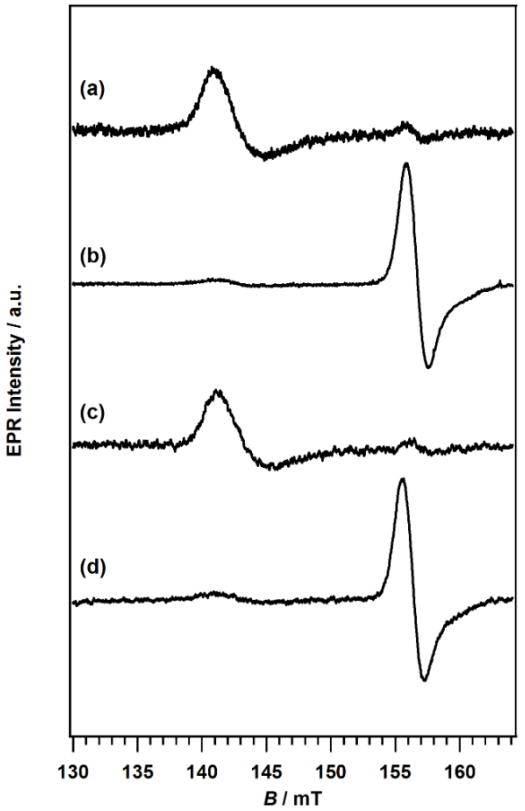

Fig. 9 EPR spectra of the $\Delta M_S = \pm 2$ transitions for the T_1 states of (a) EHS, (b) EHS^-, (c) HMS and (d) HMS^- in ethanol at 77 K. The sample solutions were prepared at a concentration of 1.5×10^{-2} mol dm^{-3}.

Photoinduced triplet EPR enhancement

In the presence of an external magnetic field $\boldsymbol{B}$, the magnetic fine structure of the triplet molecule can be described by the following spin Hamiltonian:

$$\begin{aligned} H_S &= g\mu_B \boldsymbol{B}\cdot\boldsymbol{S} + \boldsymbol{S}\cdot\boldsymbol{D}\cdot\boldsymbol{S} \\ &= g\mu_B \boldsymbol{B}\cdot\boldsymbol{S} - XS_x^2 - YS_y^2 - ZS_z^2 \\ &= g\mu_B \boldsymbol{B}\cdot\boldsymbol{S} + D[S_z^2 - (1/3)\boldsymbol{S}^2] + E(S_x^2 - S_y^2). \end{aligned} \quad (1)$$

Here, $-X$, $-Y$, and $-Z$ are the principal values of the $\boldsymbol{D}$ tensor (ZFS tensor), and D and E are the ZFS parameters. The other symbols have their usual meaning. We may assume that the g tensor is isotropic. Assuming the molecular planarity in the T_1 state, the principal axes (x, y, z) of the ZFS tensor were taken to be as shown in Scheme 1. The ZFS parameters D and E are defined to be $D = -3Z/2$ and $E = (Y - X)/2$.

The value of ZFS parameter D^* can be obtained from the observed resonance field of B_{min} signal with the aid of the following equation:[48]

$$D^* = \{(3/4)(h\nu)^2 - 3(g\mu_B B_{min})^2\}^{1/2} \quad (2)$$

where,

$$D^* = (D^2 + 3E^2)^{1/2} \quad (3)$$

h and ν have their conventional meanings. The g value was assumed to be equal to the free electron value. The transitions observed at B_{min} correspond to the transitions between two sublevels which are not adjacent at high magnetic fields. Consequently, these transitions are often called $\Delta M_S = \pm 2$ transitions.

The EPR spectra of the T_1 states of EHS, HMS, EHS^- and HMS^- were measured in ethanol at 77 K, as shown in Fig. 9 and 10. The values of D^* were obtained from the observed resonance field of B_{min} with Kottis and Lefebvre's correction and are listed in Table 1.[48] The T_1 lifetimes obtained from the decay of the EPR B_{min} signal are also listed in Table 1. The T_1 lifetimes obtained from the EPR measurements are in good agreement with those obtained from the phosphorescence measurements. This agreement shows that the observed EPR spectra are reasonably assigned to the EPR spectra of the T_1 states of EHS, HMS, EHS^- and HMS^-. The EPR spectra of the T_1 states of SA, MeS, MBA, MeMB, SA^-, MeS^- and MBA^- were measured for comparison, as shown in Fig. S4 and S6–S8.

The $\Delta M_S = \pm 1$ transition signals for EHS and HMS are too weak to be observed, as shown in Fig. 10. On the other hand, B_{min} signal and two sets of the $\Delta M_S = \pm 1$ transition signals were observed for EHS^- and HMS^-. The $\Delta M_S = \pm 1$ transition signals near 330 mT were not observed because very strong EPR signals due to free radicals formed by UV irradiation were observed over the range of the external magnetic field from 300 to 350 mT.

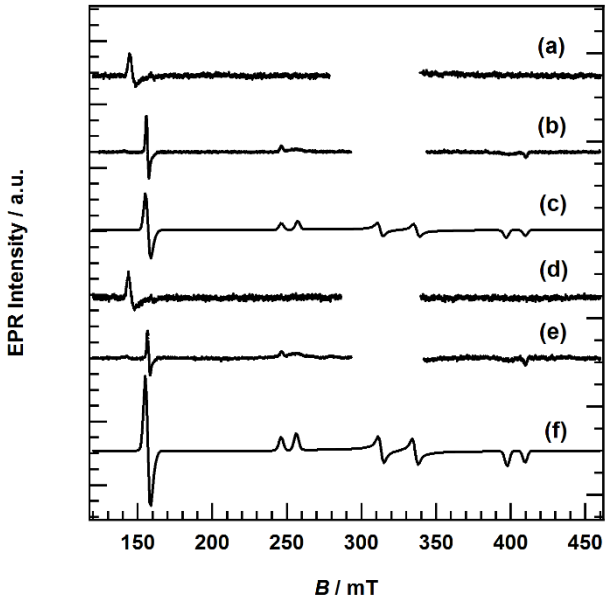

Fig. 10 EPR spectra for the T_1 states of (a) EHS, (b) EHS^-, (d) HMS and (e) HMS^- in ethanol at 77 K. The sample solutions were prepared at a concentration of 1.5×10^{-2} mol dm^{-3}. (c) Computer-simulated EPR spectrum of EHS^- obtained by using $D = 0.0763$ cm^{-1}, $E = 0.0179$ cm^{-1} and $\nu = 9221$ MHz. (f) Computer-simulated EPR spectrum of HMS^- obtained by using $D = 0.0763$ cm^{-1}, $E = 0.0184$ cm^{-1} and $\nu = 9207$ MHz.

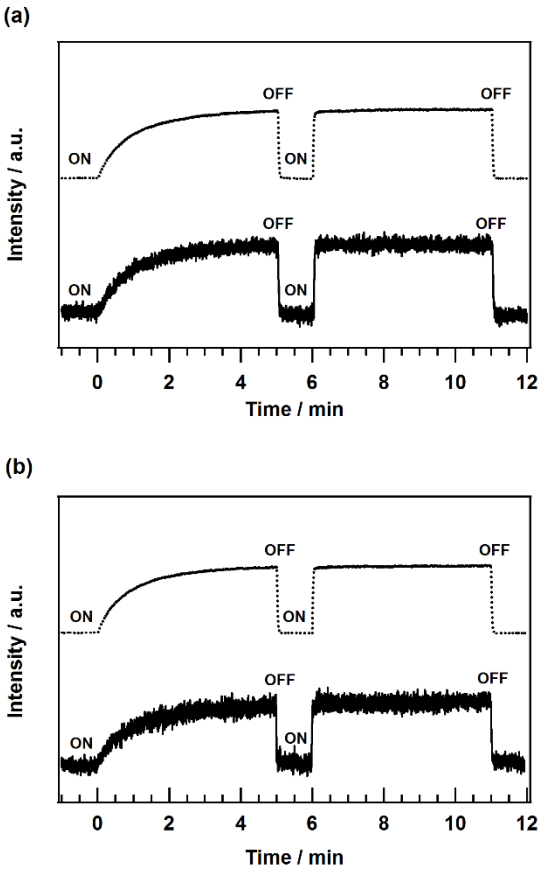

Fig. 11 Irradiation time dependence of the intensity of phosphorescence and EPR of (a) EHS and (b) HMS in ethanol at 77 K. Phosphorescence was monitored at 420 nm and EPR signal was monitored at 140.7 mT. The sample solutions were prepared at a concentration of 1.5×10^{-2} mol dm^{-3}.

The signs of the ZFS parameters of EHS^- and HMS^- are not known. We assumed that the signs of D and E are positive and $D > 3E$. The ZFS parameters thus obtained are $D = 0.0763$ cm^{-1} and $E = 0.0179$ cm^{-1} for EHS^- and $D = 0.0763$ cm^{-1} and $E = 0.0184$ cm^{-1} for HMS^-, respectively. The observed EPR spectra of the randomly oriented triplet states were simulated in the same manner as presented by Kottis and Lefebvre.[48] In the present simulation, a Gaussian linewidth of 3 mT was used. The computer-simulated EPR spectra are shown in Fig. 10.

At high magnetic fields when the three spin states are totally quantized by the magnetic field according to their M_S value and the $\Delta M_S = \pm 1$ transition is an allowed transition.[49] On the other hand, the so-called half-field transition is a forbidden transition in the sense of $\Delta M_S = \pm 2$. However, the observed B_{min} signal is much stronger than the $\Delta M_S = \pm 1$ transition signals, as shown in Fig. 10. This can be explained from the fact that in the low field of 150 mT an M_S is not a good quantum number for the spin states with ZFS parameters of ~0.1 cm^{-1} and the whole M_S quantization scheme breaks down.[49] The appearance of strong half-field transition is not a violation of the selection rule of $\Delta M_S = \pm 1$ because this rule only holds for eigenfunctions of S_z and it does not apply for the T_1 molecules studied in this work.

Fig. 11 shows the irradiation time dependence of the intensity of EPR and phosphorescence for the T_1 state of EHS. As is clearly seen in Fig. 11, the EPR intensity rose and approached to an equilibrium value. This behavior is the same as that of phosphorescence. The photoinduced enhancement of the concentration of T_1 molecules were confirmed by the phosphorescence and EPR measurements.

The lifetimes of the T_1 states of EHS and HMS are about 1 s and the D^* values are about 0.14 cm^{-1}. These values suggest that the T_1 states of EHS and HMS possess mainly a $^3\pi\pi^*$ character in ethanol. As is clearly seen in Table 1, the energy levels, lifetimes and D^* values of the T_1 states of EHS and HMS are similar to those of MeS, MBA and MeMB. The T_1 states of EHS and HMS can reasonably be assigned to a locally excited triplet state within SA molecular moiety, and the two unpaired electrons of EHS and HMS in the T_1 states localize on the SA molecular moiety.

Conclusions

The observed T_1 energies of EHS and HMS are higher than those of BMDBM and OMC, the most widely used UV-A and UV-B absorbers. EHS and HMS may act as a triplet energy donor for BMDBM and OMC in the mixtures of UV absorbers. Transient absorption and time-resolved near-IR measurements show that the $S_1 \rightarrow T_1$ intersystem crossing is not negligible for EHS and HMS in ethanol at room temperature. Photoinduced phosphorescence enhancement was observed for EHS and HMS in ethanol at 77 K. One possible explanation for the observed phosphorescence enhancement is that under irradiation the photoinduced intermolecular hydrogen-bond formation between the solute and ethanol leads to the enhancement of the $S_1 \rightarrow T_1$ intersystem crossing.

Acknowledgements

This work was supported in part by JSPS KAKENHI Grant Numbers 23241034, 24655060. This work was also supported in part by Takahashi Industrial and Economic Research Foundation.

Notes and references

[a] *Department of Chemistry, Graduate School of Engineering, Yokohama National University, Tokiwadai, Hodogaya-ku, Yokohama 240-8501, Japan. E-mail: akikuchi@ynu.ac.jp, yagimiki@ynu.ac.jp*

Electronic Supplementary Information (ESI) available: The phosphorescence and EPR spectra of SA, SA^-, MeS, MeS^-, MBA, MBA^- and MeMB in ethanol at 77 K. See DOI: 10.1039/b000000x/

1 S. Hou, W. M. Hetherington III, G. M. Korenowski and K. B. Eisenthal, Intramolecular proton transfer and energy relaxation in ortho-hydroxybenzophenone, *Chem. Phys. Lett*., 1979, **68**, 282–284.

2 M. Wiechmann, H. Port, W. Frey, F. Lärmer and T. Elsässer, Time-resolved spectroscopy on ultrafast proton transfer in 2-(2'-hydroxy-5'-methylphenyl)benzotriazole in liquid and polymer environments, *J. Phys. Chem*., 1991, **95**, 1918–1923.

3 S. J. Formosinho and L. G. Arnaut, Excited-state proton transfer reactions II. Intramolecular reactions, *J. Photochem. Photobiol., A*, 1993, **75**, 21–48.

4 C. Chudoba, E. Riedle, M. Pfeiffer and T. Elsaesser, Vibrational coherence in ultrafast excited state proton transfer, *Chem. Phys. Lett*., 1996, **263**, 622–628.

5. T. Okazaki, N. Hirota and M. Terazima, Picosecond time-resolved transient grating method for heat detection: excited-state dynamics of $FeCl_3$ and *o*-hydroxybenzophenone in aqueous solution, *J. Phys. Chem. A*, 1997, **101**, 650–655.

6 N. A. Shaath, The chemistry of ultraviolet filters, in *Sunscreens*, ed. N. A. Shaath, Taylor & Francis, Boca Raton, 2005, pp. 217–238.

7 N. A. Shaath, Ultraviolet filters, *Photochem. Photobiol. Sci*., 2010, **9**, 464–469.

8 R. Krishnan and T. M. Nordlund, Fluorescence dynamics of three UV-B sunscreens, *J. Fluoresc*., 2008, **18**, 203–217.

9 M. D. Palm and M. N. O'Donoghue, Update on photoprotection, *Dermatol. Ther*., 2007, **20**, 360–376.

10 K. Klein and I. Palefsky, Formulating sunscreen products, in *Sunscreens*, ed. N. A. Shaath, Taylor & Francis, Boca Raton, 2005, pp. 353–383.

11 D. R. Sambandan and D. Ratner, Sunscreens: An overview and update, *J. Am. Acad. Dermatol*., 2011, **64**, 748–758.

12 D. C. Steinberg, Regulations of sunscreens worldwide, in *Sunscreens*, ed. N. A. Shaath, Taylor & Francis, Boca Raton, 2005, pp. 173–198.

13 U. Osterwalder and B. Herzog, The long way towards the ideal sunscreen—where we stand and what still needs to be done, *Photochem. Photobiol. Sci*., 2010, **9**, 470–481.

14 E. Chatelain and B. Gabard, Photostabilization of butyl methoxydibenzoylmethane (avobenzone) and ethylhexyl methoxycinnamate by bis-ethylhexyloxyphenol methoxyphenyl triazine (Tinosorb S), a new UV broadband filter, *Photochem. Photobiol*., 2001, **74**, 401–406.

15 C. A. Bonda, The photostability of organic sunscreen actives: A review, in *Sunscreens*, ed. N. A. Shaath, Taylor & Francis, Boca Raton, 2005, pp. 321–349.

16 N. A. Shaath, Global developments in sun care ingredients, *Cosmet. Toiletries*, 2006, **121**, 57–66.

17 L. R. Gaspar and P. M. B. G. M. Campos, Evaluation of the photostability of different UV filter combinations in a sunscreen, *Int. J. Pharm*., 2006, **307** 123–128.

18 D. Dondi, A. Albini and N. Serpone, Interactions between different solar UVB/UVA filters contained in commercial suncreams and consequent loss of UV protection, *Photochem. Photobiol. Sci*., 2006, **5**, 835–843.

19 E. Damiani, W. Baschong and L. Greci, UV-Filter combinations under UV-A exposure: Concomitant quantification of over-all spectral stability and molecular integrity, *J. Photochem. Photobiol., B*, 2007, **87**, 95–104.

20 B. Herzog, M. Wehrle and K. Quass, Photostability of UV absorber systems in sunscreens, *Photochem. Photobiol*., 2009, **85**, 869–878.

21 C. Mendrok-Edinger, K. Smith, A. Janssen and J. Vollhardt, The quest for avobenzone stabilizers and sunscreen photostability, *Cosmet. Toiletries*, 2009, **124**, 47–54.

22 C. Bonda, A. Pavlovic, K. Hanson and C. Bardeen, Singlet quenching proves faster is better for photostability, *Cosmet. Toiletries*, 2010, **125**, 40–48.

23 V. Lhiaubet-Vallet, M. Marin, O. Jimenez, O. Gorchs, C. Trullas and M. A. Miranda, Filter-filter interactions. Photostabilization, triplet quenching and reactivity with singlet oxygen, *Photochem. Photobiol. Sci*., 2010, **9**, 552–558.

24 S. Scalia and M. Mezzena, Photostabilization effect of quercetin on the UV filter combination, butyl methoxydibenzoylmethane–octyl methoxycinnamate, *Photochem. Photobiol*., 2010, **86**, 273–278.

25 A. Kikuchi and M. Yagi, Direct observation of the intermolecular triplet-triplet energy transfer from UV-A absorber 4-*tert*-butyl-4'-methoxydibenzoylmethane to UV-B absorber octyl methoxycinnamate, *Chem. Phys. Lett*., 2011, **513**, 63–66.

26 J. Kockler, M. Oelgemöller, S. Robertson and B. D. Glass, Photostability of sunscreens. *J. Photochem. Photobiol., C*, 2012, **13**, 91–110.

27 N. Oguchi-Fujiyama, K. Miyazawa, A. Kikuchi and M. Yagi, Photophysical properties of dioctyl 4-methoxybenzylidenemalonate: UV-B absorber, *Photochem. Photobiol. Sci*., 2012, **11**, 1528–1535.

28 A. Kikuchi, N. Oguchi-Fujiyama, K. Miyazawa and M. Yagi, Triplet–triplet energy transfer from a UV-A absorber butylmethoxydibenzoylmethane to UV-B absorbers, *Photochem. Photobiol*., 2014, **90**, 511–516.

29 N. J. Turro, V. Ramamurthy and J. C. Scaiano, *Modern Molecular Photochemistry of Organic Molecules*, University Science Books, Sausalito, 2010.

30 A. Kikuchi, N. Oguchi and M. Yagi, Optical and electron paramagnetic resonance studies of the excited states of 4-*tert*-butyl-4'-methoxydibenzoylmethane and 4-*tert*-butyl-4'-methoxydibenzoylpropane, *J. Phys. Chem., A*, 2009, **113**, 13492–13497.

31 R. Kumasaka, A. Kikuchi and M. Yagi, Photoexcited states of UV absorbers, benzophenone derivatives, *Photochem. Photobiol*., 2014, **90**, 727–733.

32 T. Tsuchiya, A. Kikuchi, N. Oguchi-Fujiyama, K. Miyazawa and M. Yagi, Photoexcited triplet states of UV-B absorbers: ethylhexyl triazone and diethylhexylbutamido triazone, *Photochem. Photobiol. Sci*., 2015, 14, 807–814.

33 R. Schmidt, Solvent Shift of the $^1\Delta_g \rightarrow {}^3\Sigma_g^-$ phosphorescence of O_2, *J. Phys. Chem*., 1996, **100**, 8049–8052.

34 O. Shimizu, J. Watanabe, K. Imakubo and S. Naito, Absolute quantum yields and lifetimes of photosensitized phosphorescence of singlet oxygen O_2 ($^1\Delta_g$) in air-saturated aqueous and organic solutions of phenalenone, *Chem. Lett*., 1999, **28**, 67–68.

35 A. Kikuchi, K. Shibata, R. Kumasaka and M. Yagi, Optical and time-resolved electron paramagnetic resonance studies of the excited states of a UV-B absorber (4-methylbenzylidene)camphor, *J. Phys. Chem., A*, 2013, **117**, 1413–1419.

36 E. Oliveros, P. Suardi-Murasecco, T. Aminian-Saghafi and A. M. Braun, 1*H*-Phenalen-1-one: Photophysical properties and singlet-oxygen production, *Helv. Chim. Acta* 1991, **74**, 79–90.

37 R. Schmidt, C. Tanielian, R. Dunsbach and C. Wolff, Phenalenone, a universal reference compound for the determination of quantum yields of singlet oxygen $O_2(^1\Delta_g)$ sensitization, *J. Photochem. Photobiol., A*, 1994, **79**, 11–17.

38 A. Kikuchi, S. Yukimaru, N. Oguchi, K. Miyazawa and M. Yagi, Excited triplet state of a UV-B absorber, octyl methoxycinnamate, *Chem. Lett*., 2010, **39**, 633–635.

39 M. Aleksiejew and J. R. Heldt, Experimental and theoretical studies of electronic energy states of methyl benzoate derivatives, *J. Lumin*., 2007, **126**, 665–676.

40 F. Waiblinger, J. Keck, M. Stein, A. P. Fluegge, H. E. A. Kramer and D. Leppard, Light-induced opening of the intramolecular hydrogen bond of UV absorbers of the 2-(2-hydroxyphenyl)-1,3,5-triazine and the 2-(2-hydroxyphenyl)benzotriazole type. *J. Phys. Chem., A*, 2000, **104**, 1100–1106.

41 F. Waiblinger, A. P. Fluegge, J. Keck, M. Stein, H. A. Kramer and D. Leppard, Irradiation-dependent equilibrium between open and closed form of UV absorbers of the 2-(2-hydroxyphenyl)-1,3,5-triazine type, *Res. Chem. Intermed*., 2001, **27**, 5–20.

42 A. P. Fluegge, F. Waiblinger, M. Stein, J. Keck, H. E. A. Kramer, P. Fischer, M. G. Wood, A. D. DeBellis, R. Ravichandran and D. Leppard, Probing the intramolecular hydrogen bond of 2-(2-hydroxyphenyl)benzotriazoles in polar environment: a photophysical study of UV absorber efficiency. *J. Phys. Chem., A*, 2007, **111**, 9733–9744.

43 T. P. Carsey, G. L. Findley and S. P. McGlynn, Systematics in the electronic spectra of polar molecules. 1. Para-disubstituted benzenes, *J. Am. Chem. Soc*., 1979, **101**, 4502–4510.

44 G. Heinrich, S. Schoof and H. Gusten, 9,10-Diphenylanthracene as a fluorescence quantum yield standard, *J. Photochem*., 1974–1975, **3**, 315–320.

45 M. Montalti, A. Credi, L. Prodi and M. T. Gandolfi, *Handbook of photochemistry, 3rd ed*., Tayler & Francis, Boca Raton, 2006.

46 A. Kikuchi, K. Shibata, R. Kumasaka and M. Yagi, Excited states of menthyl anthranilate: a UV-A absorber, *Photochem. Photobiol. Sci*., 2013, **12**, 246–253.

47 A. Kikuchi, Y. Hata, R. Kumasaka, Y. Nanbu and M. Yagi, Photoexcited singlet and triplet states of a UV absorber ethylhexyl methoxycrylene, *Photochem. Photobiol*., 2013, **89**, 523–528.

48 P. Kottis and R. Lefebvre, Calculation of the electron spin resonance line shape of randomly oriented molecules in a triplet state. I. The $\Delta m = 2$ transition with a constant linewidth, *J. Chem. Phys*., 1963, **39**, 393–403.

49 A. Carrington, A. D. McLachlan, *Introduction to magnetic resonance*, Harper & Row, New York, 1967.